Research Article

An evaluation of cellulose saccharification and fermentation with an engineered *Saccharomyces cerevisiae* capable of cellobiose and xylose utilization

Jerome M. Fox[1,2], *Seth E. Levine*[1,2], *Harvey W. Blanch*[2] *and Douglas S. Clark*[2]

[1] Energy Biosciences Institute University of California, Berkeley, CA, USA
[2] Department of Chemical and Biomolecular Engineering, University of California, Berkeley, CA, USA

Commercial-scale cellulosic ethanol production has been hindered by high costs associated with cellulose-to-glucose conversion and hexose and pentose co-fermentation. Simultaneous saccharification and fermentation (SSF) with a yeast strain capable of xylose and cellobiose co-utilization has been proposed as a possible avenue to reduce these costs. The recently developed DA24-16 strain of *Saccharomyces cerevisiae* incorporates a xylose assimilation pathway and a cellodextrin transporter (CDT) that permit rapid growth on xylose and cellobiose. In the current work, a mechanistic kinetic model of cellulase-catalyzed hydrolysis of cellulose was combined with a multi-substrate model of microbial growth to investigate the ability of DA24-16 and improved cellobiose-consuming strains to obviate the need for exogenously added β-glucosidase and to assess the impact of cellobiose utilization on SSF and separate hydrolysis and fermentation (SHF). Results indicate that improved CDT-containing strains capable of growing on cellobiose as rapidly as on glucose produced ethanol nearly as rapidly as non-CDT-containing yeast supplemented with β-glucosidase. In producing 75 g/L ethanol, SSF with any strain did not result in shorter residence times than SHF with a 12 h saccharification step. Strains with improved cellobiose utilization are therefore unlikely to allow higher titers to be reached more quickly in SSF than in SHF.

Received	18 JUL 2011
Revised	19 DEC 2011
Accepted	29 DEC 2011
Accepted article online	09 JAN 2012

Supporting information available online

Keywords: Biochemical engineering · Biofuels · Cellobiose · Cellulose · *Saccharomyces*

See accompanying Commentary by Jin and Cate DOI: 10.1002/biot.201100489

1 Introduction

Cellulosic biofuels may provide a viable low-carbon alternative to traditional fossil fuels, but high cellulose-to-sugar conversion costs and inefficient fermentation of both hexose and pentose sugars have made commercial production economically unattractive. Simultaneous saccharification and fermentation (SSF) has been proposed as a possible avenue to improve process economics. In this one-reactor scenario, cellulase enzymes catalyze the hydrolysis of cellulose to glucose, which is simultaneously fermented into alcohols or other liquid fuels, thus preventing monomeric sugars and soluble cello-oligosaccharides from inhibiting the enzymatic polymerization process. Alcohols produced during SSF have the potential to reduce microbial contamination that might occur in non-aseptic saccharification reactors, and the use of one reactor has been proposed as a possible strategy to lower equipment costs [1–3].

Yeast strains capable of simultaneous cellodextrin and xylose fermentation may be particularly

Correspondence: Prof. Douglas S. Clark, Department of Chemical and Biomolecular Engineering, 491 Tan Hall, University of California, Berkeley, CA 94720-1462, USA
E-mail: clark@berkeley.edu
Additional correspondence: Dr. Harvey W. Blanch
E-mail: blanch@berkeley.edu

Abbreviations: CBH, cellobiohydrolase; **CDT**, cellodextrin transporter; **SHF**, separate hydrolysis and fermentation; **SSF**, simultaneous saccharification and fermentation

advantageous in SSF processes. The plant cell wall of biofuel-candidate grasses and trees contains xylose and glucose polymers that must be broken down into their constituent sugars prior to being metabolized into useful fuels [4]. Xylose is present primarily as the hemicellulose xylan, which is released as soluble xylose oligomers during pretreatment of lignocellulosic substrates [5, 6]. Glucose is present in the β-1,4-linked cellobiose polymer cellulose, which undergoes saccharification through an enzyme-catalyzed hydrolysis process that takes place after pretreatment. The cellulase enzymes responsible for saccharification are inhibited by cellobiose; β-glucosidase is often added to alleviate this inhibition by converting cellobiose to glucose [7]. Ideally, fuel-producing microbes would be capable of using both xylose and glucose; the additional ability to consume cellobiose may obviate the need for the addition of β-glucosidase.

The engineered DA24-16 strain of *Saccharomyces cerevisiae* may improve the economics of SSF. In this strain, a xylose assimilation pathway, a *Neurospora crassa* cellodextrin transporter (CDT), and an intracellular β-glucosidase were introduced to facilitate rapid consumption of xylose and cellobiose [8]. Previous attempts to engineer xylose assimilation pathways into *S. cerevisiae* have been successful, but DA24-16 is able to grow on xylose at rates nearly equivalent to those of *Pichia stipitis*, which natively consumes xylose more rapidly than any other wild type yeast strain yet discovered [8–11]. *S. cerevisiae* strains capable of growth on cellobiose have also been engineered previously, but all have relied on secreted β-glucosidase enzymes to hydrolyze cellobiose to glucose [12–14]. The advantage of the CDT-containing DA24-16 strain relates to its ability to avoid extracellular production of glucose, which inhibits xylose consumption [15]. By obviating the need for exogenous β-glucosidase and by facilitating the uninhibited metabolism of xylose, the DA24-16 *S. cerevisiae* strain and yeast with similar capabilities may reduce enzyme costs and increase the sugar conversion efficiencies associated with SSF processes.

In the current work, we explore the potential advantages of cellobiose utilization by employing a mechanistic kinetic model of cellulase action and a multi-substrate model of microbial growth to compare the performance of a CDT-containing strain in SSF to the performance of a non-CDT-containing strain in SSF and separate hydrolysis and fermentation (SHF). Our analysis places particular emphasis on assessing the capacity of cellobiose transporters acting in concert with an intracellular β-glucosidase to replace exogenously added β-glucosidase enzymes in the hydrolysis process, and on evaluating the impact of cellobiose utilization on the possible advantages of SSF over SHF. Xylose growth parameters for both strains and cellobiose growth parameters for the cellodextrin-containing strain were equated to those of DA24-16; however, our results are generally applicable to other CDT-containing *S. cerevisiae* strains that are able to consume multiple substrates. The sensitivity of our results to these parameters and the likelihood of altered growth behavior in response to changes in these parameters are also discussed. This work marks the first time that an independently validated mechanistic model of cellulase action capable of tracking cello-oligosaccharide chain length has been used alongside a microbial growth model to assess the potential benefits of cellobiose consumption in yeast.

2 Materials and methods

2.1 Choice of enzymatic hydrolysis conditions

The process economics of commercial-scale cellulosic biofuels production are enhanced by high solids loadings (20% or higher), which lower energy costs associated with substrate flow and product separation [16]. In the present work, commercial operation requirements were accommodated through the use of cellulose and xylose concentrations of 129 and 71 g/L, respectively. These match the average cellulose/xylan ratio (15:9) of candidate biofuels crops and amount to a 200 g/L (20%) solids loading in reactions where both substrates are present [4]. This solids loading refers to the pretreated slurry where the lignin has been removed [16].

The cellulase enzymes chosen for this study were *Trichoderma* sp. Cel7A (*Tr*Cel7A), *Trichoderma* sp. Cel6A (*Tr*Cel6A), and *Talaromyces emersonii* GH5 (*Tem*GH5). These fungal cellulases are similar to the main constituents of commercial cellulase mixtures. The *Tr*Cel7A and *Tr*Cel6A cellobiohydrolases (CBHs) catalyze the hydrolysis of insoluble cellulose by adsorbing to the substrate, complexing with reducing ends (*Tr*Cl7A) or non-reducing ends (*Tr*Cel6A) of cellulose chains, engaging in processive catalysis, decomplexing from chains, and recomplexing or desorbing from the surface. The *Tem*GH5 endoglucanase enzyme engages in a similar manner, but complexes anywhere within chains and catalyzes only one hydrolysis event before decomplexing. In solution, all three enzymes can directly hydrolyze soluble cello-oligosaccharides (DP < 7). The kinetics of these steps are de-

scribed by Levine et al. [17, 32], and parameter values are included in Supporting information, Table S1. Cellulose was assumed to have the properties of Avicel, as described by Levine et al [17].

In our studies, xylose was used as a surrogate for the xylan hydrolyzate produced during pretreatment of lignocellulosic substrates. Pretreatments such as dilute acid hydrolysis, alkaline hydrolysis, steam explosion, liquid hot water pretreatment, and ionic liquid pretreatment can remove the majority of xylan from cellulosic substrates, producing xylose and a variety of soluble xylo-oligomers [5, 6, 18, 19]. These xylo-oligomers, which can make up over 50% of xylan hydrolyzate, have been shown to inhibit cellulase activity as strongly as cellobiose, which is about 100-fold more inhibitory than glucose. Xylo-oligomer concentrations, however, can be significantly reduced and converted to xylose by optimized pretreatment processes or through the addition of β-D-xylosidase to hydrolysis reactions [20–22]. Accordingly, xylan hydrolyzate is represented as xylose in the present work. Xylose is thought to be a competitive inhibitor of cellulase enzymes [5, 23]; however, there are no directly measured xylose inhibition parameters available in the literature. In the present work, these parameters were equated with the glucose inhibition parameters for each enzyme ($K_{i\text{–EG–G}} = K_{i\text{–EG–Xy}}$). Pretreatments that incompletely hydrolyze xylan, creating a requirement for significant xylanase action during the cellulose hydrolysis step, are not addressed here.

Pretreatments that hydrolyze the majority of the hemicellulose produce xylose feed streams that that can be routed either to glucose/xylose co-fermentation reactors or to separate xylose fermentation units [18, 24]. Process scenarios in which xylose undergoes a separate fermentation step are not addressed in the present work. In our model, xylan hydrolyzate is included in the combined hydrolysis and fermentation of SSF, whereas in SHF, it is included in the fermentation but not necessarily in the hydrolysis reaction.

Cellulase loadings of 25 mg enzyme/g glucan were used in each simulation. This loading is similar to that reported for proposed commercial operations and to those employed in recently-published SSF studies [25–28]. The cellulase mixture contained cellobiohydrolase I (CBHI), cellobiohydrolase II (CBHII), and endoglucanase (EGI) in a 1:3:1 molar ratio, which is close to the optimal composition reported for these enzymes [29]. When β-glucosidase was present, it represented 10% of the total enzyme concentration (by mass), a commonly reported β-glucosidase concentration [21].

The optimal conditions for the fungal enzymes considered are pH of 4.85 and a temperature of 50°C. The growth and ethanol production rates of *S. cerevisiae* are highest at a pH of 5.5 and a temperature of 30°C. Previous studies have shown the activity of *Trichoderma* sp. enzymes to be 50% lower at 30°C than at 50°C [30]. We therefore accounted for the reduction in enzyme activity at 30°C by reducing the cellulase enzyme k_{cat} values by 50%. The effect of pH 5.5 on optimal enzyme activity is small (<5% reduction in activity) [30], and was ignored in this work. The kinetic parameters for β-glucosidase activity at 30 and 50°C were taken directly from Chauve et al [31]. All other parameters were obtained from the literature and were assumed to be independent of temperature in the 30–50°C range (Supporting information, Table S1).

2.2 Hydrolysis model development

Cellulose saccharification was modeled with the mechanistic kinetic model of cellulase-catalyzed hydrolysis recently developed by Levine et al [32]. Cellulase action on insoluble cellulosic substrates is modeled as a heterogeneous biocatalytic reaction involving endo- and exocellulases that either interact directly with soluble cello-oligosaccharides (DP < 7) or form complexes with insoluble cellulose chains after first adsorbing to available sites on the substrate surface. Unlike previously developed models of cellulase catalysis, this model tracks all chain lengths and products, and it does not assume equilibrium for CBH-substrate complexes [32–36]. This model also explicitly accommodates the reduced activity by endoglucanase enzymes at chain ends, and processive catalysis by CBH enzymes along chains.

The action of beta-glucosidase on cellobiose was modeled with Michaelis–Menten kinetics modified to include competitive inhibition by glucose:

$$\frac{d[C_2]}{dt} = \frac{k_{cat\text{–BG–}C_2}\,BG[C_2]}{[C_2] + K_{M\text{–BG–}C_2}\left(1 + \frac{[C_1]}{K_{i\text{–BG–}C_1}}\right)} \quad (1)$$

where BG is the concentration of β-glucosidase and $K_{i\text{–BG–}C_1}$ is the equilibrium constant for competitive inhibition by glucose.

For SSF, the additional influences of ethanol and xylose on enzyme behavior were incorporated through the addition of non-competitive and competitive inhibition terms, which were obtained from reports on the effect of these compounds on cellulose hydrolysis rates [5, 37]. These terms appear in equations for the site and enzyme balances. Inhibi-

tion effects of ethanol and xylose were described by the following relationships:

$$k_{\text{cat}}^{\text{app}} = \frac{k_{\text{cat}}}{1 + \dfrac{[\text{Eth}]}{K_{i-\text{Eth}}}} \tag{2}$$

$$K_{\text{M}}^{\text{app}} = K_{\text{M}} \left(\begin{array}{l} 1 + \displaystyle\sum_{i=7}^{\infty} \frac{\theta_{\text{CBH1}}[C_i']}{K_{\text{M-CBH1-cel}}} + \sum_{i=3}^{6} \frac{[C_i]}{K_{\text{M-CBH1-sol}}} \\ + \dfrac{[C_1]}{K_{i-\text{CBH1-}C_1}} + \dfrac{[C_2]}{K_{\text{M-CBH1-}C_2}} \\ + \dfrac{[\text{Xy}]}{K_{i-\text{CBH1-Xy}}} \end{array} \right) \tag{3}$$

where k_{cat} represents an arbitrary kinetic constant, and $K_{i-\text{Eth}}$ represents the noncompetitive equilibrium constant between ethanol and a given enzyme. The other parameters are defined as in Levine et al. [17, 32]; their values are reported in Supporting information, Table S1.

2.3 Choice of SSF and SHF conditions

Our comparisons of SSF and SHF processes are based on the total residence times required to reach particular ethanol concentrations. Estimates of the combined residence time for hydrolysis and fermentation processes range from 3 to 6 days, but 2–3 day targets have been proposed for commercial operations [38]. For SHF, we considered three different hydrolysis times spanning the period over which the hydrolysis rate varied significantly (Fig. 1): 12, 24, and 36 h.

Fermentations were simulated at the optimal pH and temperature for growth and ethanol production by *S. cerevisiae* (pH = 5.5; T = 30°C). When fermentation and hydrolysis were conducted separately, they were done so under pH and temperature conditions that were optimal for each step: pH 4.85 and 50°C for saccharification and pH 5.5 and 30°C for fermentation. Fermentations were modeled with and without xylose to assess the impact of this sugar on the results.

All fermentations had an inoculum of 0.252 g cells/L (OD_{600} ~ 1.0) so that growth could be compared with published batch fermentation processes. The impact of larger inocula on residence times is addressed below.

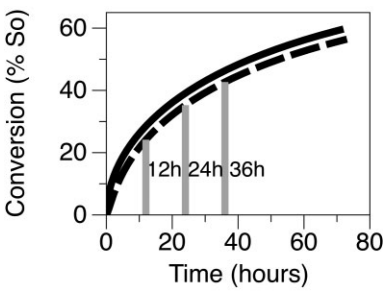

Figure 1. Profiles of cellulose conversion during saccharification reactions. Runs were carried out for 144 h at 50°C with a combined total enzyme loading of 2.5 g/L and substrate concentrations of 128.57 g/L cellulose with or without 71.43 g/L xylose. Cellulases were present in a 1:3:1 EG2/CBH1/CBH2 (molar) enzyme ratio; β-glucosidase made up 10% of the enzyme mixture by mass. Solid black line (cellulose present); dashed black line (cellulose and xylose present).

2.4 Model development for SSF and SHF

Yeast growth was modeled using Monod kinetics with growth-associated ethanol production and threshold-based ethanol inhibition. Simultaneous utilization of multiple carbon sources (glucose, cellobiose, and xylose) was incorporated through additive growth kinetics modified to include catabolic repression of cellobiose and xylose utilization by glucose. Previous reports on the DA24-16 strain showed no evidence that xylose inhibits cellobiose uptake or vice versa. The resulting equation for batch growth in the absence of cellulases is identical in form to that proposed for the glucose, cellobiose, and xylose fermenting yeast *Candida lusitaniae* [39]:

$$\frac{dX}{dt} = \left(\begin{array}{l} \dfrac{\mu_{\max-C_1} C_1}{K_{C_1} + C_1} + \dfrac{\mu_{\max-C_2} C_2}{K_{C_2} + C_2} \dfrac{1}{B_{i-C_1-C_2} C_1 + 1} \\ + \dfrac{\mu_{\max-\text{Xy}} \text{Xy}}{K_{\text{Xy}} + \text{Xy}} \dfrac{1}{B_{i-C_1-\text{Xy}} C_1 + 1} \end{array} \right) \left(1 - \frac{[\text{Ethanol}]}{K_{i-\text{Eth}-X}} \right) X \tag{4}$$

Ethanol production by each substrate was modeled in an analogous fashion:

$$\frac{d\text{Eth}}{dt} = \left(\begin{array}{l} \dfrac{Y_{\text{Eth}/C_1}}{Y_{X/C_1}} \dfrac{\mu_{\max-C_1} C_1}{K_{C_1} + C_1} \\ + \dfrac{Y_{\text{Eth}/C_2}}{Y_{X/C_2}} \dfrac{\mu_{\max-C_2} C_2}{K_{C_2} + C_2} \dfrac{1}{B_{i-C_1-C_2} C_1 + 1} \\ + \dfrac{Y_{\text{Eth/Xy}}}{Y_{X/\text{Xy}}} \dfrac{\mu_{\max-\text{Xy}} \text{Xy}}{K_{\text{Xy}} + \text{Xy}} \dfrac{1}{B_{i-C_1-\text{Xy}} C_1 + 1} \end{array} \right) \left(1 - \frac{[\text{Ethanol}]}{K_{i-\text{Eth}-X}} \right) X \tag{5}$$

Uptake equations for each carbon source were based on Monod kinetics:

$$\text{rate of glucose uptake} = -\left(\frac{1}{Y_{X/C_1}} \right) \left(\frac{\mu_{\max-C_1} C_1}{K_{C_1} + C_1} \right) \left(1 - \frac{[\text{Ethanol}]}{K_{i-X-\text{Eth}}} \right) X \tag{6}$$

$$\text{rate of cellobiose uptake} = -\left(\frac{1}{Y_{X/C_2}}\right)\left(\frac{\mu_{\max-C_2}C_2}{K_{C_2}+C_2}\right)\left(\frac{1}{B_{i-C_1-C_2}C_1+1}\right)\left(1-\frac{[\text{Ethanol}]}{K_{i-\text{Eth}-X}}\right)X \quad (7)$$

$$\text{rate of xylose uptake} = -\left(\frac{1}{Y_{X/\text{Xy}}}\right)\left(\frac{\mu_{\max-\text{Xy}}\text{Xy}}{K_{\text{Xy}}+\text{Xy}}\right)\left(\frac{1}{B_{i-C_1-\text{Xy}}C_1+1}\right)\left(1-\frac{[\text{Ethanol}]}{K_{i-\text{Eth}-X}}\right)X \quad (8)$$

where Y, $\mu_{\max}$, and K represent the specific yield coefficient, maximum specific growth rate, and Monod constant for growth on each substrate; B_{i-C_1} and $K_{i-\text{Eth}}$ represent parameters describing glucose inhibition of substrate uptake and ethanol inhibition of cell growth.

Equations (6) and (7) were included in the material balance for glucose and cellobiose, effectively linking the fermentation model to the cellulose hydrolysis model. Equation (8) was included in the xylose material balance.

2.5 Model parameters

To estimate values of K_{C_2}, $\mu_{\max-C_2}$, K_{Xy}, and $\mu_{\max-\text{Xy}}$ for the DA24-16 strain, the IMSL nonlinear optimizer NNLPF was used to fit batch reactor material balance equations consistent with the conditions employed by Ha et al. [8]:

$$\frac{dC_2}{dt} = -\left(\frac{1}{Y_{X/C_2}}\right)\left(\frac{\mu_{\max-C_2}C_2}{K_{C_2}+C_2}\right)\left(1-\frac{[\text{Ethanol}]}{K_{i-\text{Eth}-X}}\right)X \quad (9)$$

$$\frac{d\text{Xy}}{dt} = -\left(\frac{1}{Y_{X/\text{Xy}}}\right)\left(\frac{\mu_{\max-\text{Xy}}\text{Xy}}{K_{\text{Xy}}+\text{Xy}}\right)\left(1-\frac{[\text{Ethanol}]}{K_{i-\text{Eth}-X}}\right)X \quad (10)$$

Initial cellobiose and xylose concentrations were set at their reported experimental values of 40 g/L. Inhibition of *S. cerevisiae* growth by ethanol was assumed to be independent of substrate, so the previously measured value of $K_{i-\text{Eth}-X}$ = 87 g/L was employed [37]; the Monod constants (K_{C_1} and K_{C_2}) and maximum specific growth rates ($\mu_{\max-C_1}$ and $\mu_{\max-C_2}$) were treated as adjustable parameters and optimized. The number of available data points was low (7 total), which increased the uncertainty associated with the fitted values.

After $\mu_{\max-\text{Xy}}$ was determined, the xylose yield coefficient was estimated from the $q_{\max-\text{Xy}}$ value reported for the DA24-16 strain according to the following equation [8]:

$$q_{\max-\text{Xy}} = \frac{\mu_{\max-\text{Xy}}}{Y_{X/\text{Xy}}} \quad (11)$$

2.6 Model assembly and solution

The model was constructed in Fortran 95 using the Absoft Pro Fortran v11 compiler. The model used the IMSL function DASPG differential and algebraic equation solver, which employs the Petzold-Gear method. To capture hydrolysis and fermentation, 5365 differential equations and 15 algebraic equations from the original hydrolysis model, modified to include xylose and ethanol inhibition, were supplemented with three differential equations to track cell density, ethanol concentration, and xylose concentration.

3 Results and discussion

3.1 The potential of CDT yeast strains to reduce β-glucosidase requirements

Previous reports on cellobiose-consuming yeast have asserted that such strains may be able to alleviate cellobiose inhibition of cellulase and thereby obviate the need for exogenously added β-glucosidase enzymes, which account for up to 10% of the total enzyme cost [8, 40]. The capacity of the CDT to remove cellobiose as quickly as extracellular β-glucosidase hydrolyzes it to glucose was investigated in separate SSF reactions (Table 1; reactions 1–4). Time-course profiles of cellulose conversion into products for each of these conditions are plotted in Fig. 2A. With cellulose alone, SSF with the CDT-containing strain resulted in 10% conversion of cellulose in 140 h. In contrast, SSF with the non-CDT-containing strain supplemented with β-glucosidase achieved nearly 100% conversion in 90 h. Interestingly, when xylose was added, the CDT-containing strain achieved 25% cellulose conversion in 140 h; growth on xylose led to higher concentrations of yeast, which facilitated faster overall cellobiose uptake (see Eq. 6), reducing its inhibitory effect. The DA24-16 strain does not remove cellobiose as quickly as a non-CDT-containing strain that is supplemented with β-glucosidase, and is therefore less effective in alleviating cellobiose inhibition of cellulase-catalyzed hydrolysis.

Both xylose and cellobiose transporters are inhibited by glucose [8, 39]. To address the inhibitory effect of glucose on the cellobiose consumption rates in SSF, we examined a situation in which glucose inhibition of cellobiose and xylose uptake by the CDT-containing yeast was removed (runs 5 and

Table 1. Total residence times to achieve target ethanol concentrations within various process scenarios

Run	Process scenarios	τ_{res} (h) 40 g/L ethanol	τ_{res} (h) 75 g/L ethanol
1	SSF with CDT-containing yeast; cellulose present	>144	>144
2	SSF with CDT-containing yeast; cellulose and xylose present	>144	>144
2′	SSF with CDT-containing yeast with K_{C_1} = 0.14 mM; cellulose and xylose present	>144	>144
3	SSF with non-CDT-containing yeast supplemented with β-glucosidase; cellulose present	21.25	89
4	SSF with non-CDT-containing yeast supplemented with β-glucosidase; cellulose and xylose present	37.5	71
4′	SSF with non-CDT-containing yeast supplemented with β-glucosidase; K_{C_1} = 0.14 mM; cellulose and xylose present	26.5	56.75
5	SSF with CDT-containing yeast with no glucose inhibition of xylose and cellobiose transport; cellulose present	>144	>144
6	SSF with CDT-containing yeast with no glucose inhibition of xylose and cellobiose transport; cellulose and xylose present	>144	>144
7	SSF with CDT-containing yeast where $K_{C_1} = K_{C_2}$; cellulose present	70.5	>144
8	SSF with CDT-containing yeast where $K_{C_1} = K_{C_2}$; cellulose and xylose present	35.5	102.75
9	SSF CDT-containing yeast where $\mu_{max-C_2} = \mu_{max-C_1}$; cellulose present	>144	>144
10	SSF CDT-containing yeast where $\mu_{max-C_2} = \mu_{max-C_1}$; cellulose and xylose present	>144	>144
11	SSF CDT-containing yeast where $K_{C_2} = K_{C_1}$ and $\mu_{max-C_2} = \mu_{max-C_1}$; cellulose present	63.5	>144
12	SSF CDT-containing yeast where $K_{C_2} = K_{C_1}$ and $\mu_{max-C_2} = \mu_{max-C_1}$; cellulose and xylose present	34.5	96.75
13	SHF with 12 h hydrolysis step; xylose added in fermentation	31.5	59.5
13′	SHF with 12 h hydrolysis step; K_{C_1} = 0.14 mM; xylose added in fermentation	28	54.75
14	SHF with 12 h hydrolysis step; K_{C_1} = 0.14 mM; xylose added in hydrolysis	32.75	61.25
15	SHF with 24 h hydrolysis step; xylose added in fermentation	40.5	67.25
16	SHF with 24 h hydrolysis step; xylose added in hydrolysis	41.5	68.5
17	SHF with 36 h hydrolysis step; xylose added in fermentation	50.75	76.5
18	SHF with 36 h hydrolysis step; xylose added in hydrolysis	51.5	77.75
19	SSF CDT-containing yeast where K_{C_2} = 0 mM, $\mu_{max-C_2} = \mu_{max-C_1}$, and B_{C_1} = 0; cellulose and xylose	28.5	62.25
19′	SSF CDT-containing yeast where K_{C_2} = 0 mM, $\mu_{max-C_2} = \mu_{max-C_1}$, and $B_{C_1-C_2}$ = 0; K_{C_1} = 0.14 mM; cellulose and xylose	25	58

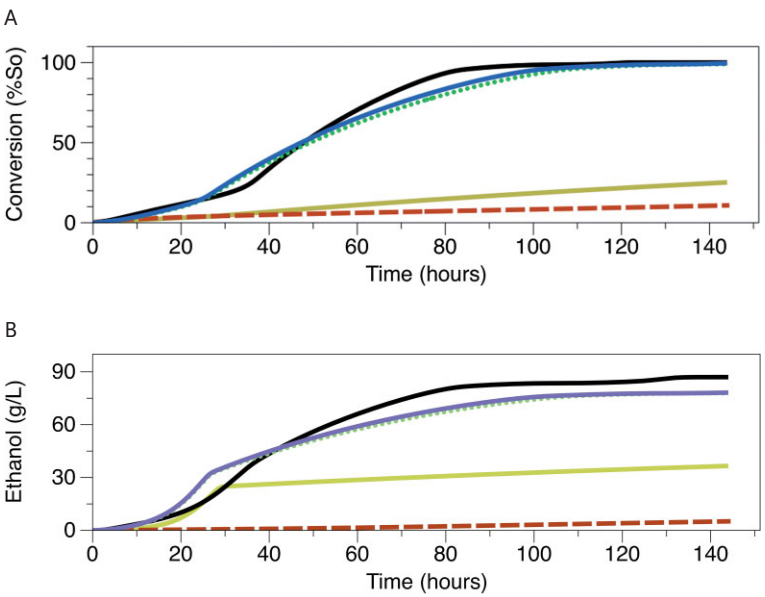

Figure 2. Profiles of cellulose hydrolysis and ethanol production in SSF scenarios. Runs were carried out for 144 h at 30°C with a 1:3:1 EG2/CBH1/CBH2 (molar) enzyme ratio, a combined total enzyme loading of 2.5 g/L, and substrate concentrations of 129 g/L cellulose with or without 71 g/L xylose. When β-glucosidase was present, it comprised 10% of the total enzyme mass. Cultures were started with a yeast inoculum of 0.252 g/L, corresponding to an OD_{600} of approximately 1. Runs are annotated with the following abbreviations: SSF; CDT and intracellular β-glucosidase present (CDT); cellulose present (C); xylose present (X). Lines show time course profiles of (**A**) cellulose conversion to products and (**B**) ethanol production for the following conditions: SSF CDT C (dashed red line, run 1); SSF CDT C X (solid yellow line, run 2); SSF CDT w/$K_{C_2} = K_{C_1}$ C X (dotted green line, run 8); SSF CDT w/$K_{C_2} = K_{C_1}$, $\mu_{max-C_2} = \mu_{max-C_1}$ C X (solid blue line, run 12); SSF C X BG (solid black line, run 4). Note: lines for runs 9 and 10 are coincident with those from runs 1 and 2, respectively.

6, Table 1). These scenarios brought about only a slight increase in cellulose conversion rates. After 144 h, SSF with CDT strains uninhibited by glucose inhibition of cellobiose uptake allowed cellulose conversion to reach 11.4 and 25.9% for runs 5 and 6, respectively; this is a 5 and 3% increase over runs 1 and 2. Clearly, in these hydrolysis scenarios, glucose was consumed nearly as rapidly as it was generated, failing to reach strongly inhibitory levels.

S. cerevisiae strains capable of cellobiose assimilation could be engineered to have faster rates of cellobiose uptake through improvements to the transporter protein or through modifications to the assimilation pathway. Enhancements in cellobiose uptake rates likely to result from such efforts were investigated by varying the kinetic parameters associated with growth of *S. cerevisiae* on cellobiose.

For the DA24-16 strain, the Monod constant for cellobiose (K_{C_2} = 350 mM) is about 200-fold larger than the analogous constant for glucose (K_{C_1} = 1.7 mM). The influence of K_{C_2} on the ability of cellobiose-utilizing *S. cerevisiae* to alleviate cellobiose inhibition of cellulase enzymes was investigated with SSF runs in which it was set equal to K_{C_1} (runs 7 and 8, Table 1). This lower value of K_{C_2} enabled cellobiose consumption to increase rates of cellulose hydrolysis almost as effectively as the addition of β-glucosidase (Fig. 2A).

The impact of increasing the specific growth rate of the CDT-containing yeast in SSF was assessed with simulations where $\mu_{max\text{–}C_2}$ was increased to $\mu_{max\text{–}C_1}$ (runs 9 and 10, Table 1). This change did not allow for faster conversion rates in SSF; conversion profiles for runs 9 and 10 were coincident with those of runs 1 and 2. This maximum specific growth rate is the highest measured for *S. cerevisiae*; it is likely limited by the maximal rate of rRNA synthesis in this yeast, not glucose uptake capacity, and is therefore independent of the nature of the substrate [41–44]. Higher values of $\mu_{max\text{–}C_2}$ were not investigated. As illustrated in Fig. 2A and B, cellulose conversion and ethanol production results for the DA24-16 strain were insensitive to the increase in $\mu_{max\text{–}C_2}$.

The influence of a faster specific growth rate was also investigated in simulations where K_{C_2} and $\mu_{max\text{–}C_2}$ were set equal to K_{C_1} and $\mu_{max\text{–}C_1}$ (runs 11 and 12, Table 1). At 72 h, when compared to run 8 (with the CDT-containing yeast with $K_{C_2} = K_{C_1}$), run 12 showed a 4.6% improvement in conversion (Fig. 2A) and a 3% improvement in ethanol concentration (Fig. 2B). Thus, only when K_{C_2} was set to K_{C_1} did an increase in the maximum specific growth rate lead to slight increases in hydrolysis rates and ethanol titers.

In practice, it may be possible to reduce K_{C_2} by enhancing the affinity of the transporter for cellobiose, by increasing the number of transporters per cell, or by raising V_{max} for the transporter enzyme [45, 46]. The *N. crassa* transporter incorporated into the DA24-16 strain has high affinity for cellobiose (apparent K_M equal to ~3 μM), which is low compared to other substrate transporters; hence, improving affinity of the transporter for cellobiose is not likely to lower K_{C_2} [8]. Transporter abundance in the membrane or activity are more likely to be effective targets for improvement.

Improvements to downstream enzymes may also lower K_{C_2}. After an intracellular hydrolysis step, the cellobiose assimilation pathway is identical to that of glucose assimilation. Thus, the activity of intracellular β-glucosidase could also be a limiting factor in cellobiose consumption.

3.2 Impact of co-utilizing cellobiose, xylose, and glucose on SSF versus SHF

The impact of cellobiose utilization on SSF and SHF was explored by comparing residence times required to achieve 40 and 75 g/L ethanol titers (Table 1). Kinetic parameters for xylose utilization were held constant in all runs (K_{xyl} and $\mu_{max\text{–}xyl}$ of the DA24-16 strain) and growth parameters for CDT-containing and non-CDT-containing yeast were identical. For all SHF runs, the residence times included in Table 1 represent the sum of the times required for hydrolysis and fermentation.

Regardless of ethanol titer, the SHF process with the 12 h hydrolysis step led to the shortest residence times: 31.5 h for 40 g/L and 59.5 h for 75 g/L. These times are 8 and 18% shorter than the shortest SSF residence times for the processes considered in Table 1.

The rankings of total residence times for the SSF scenarios depended on the ethanol titers that were targeted (Table 1). For 40 g/L ethanol, the shortest SSF residence time (34.5 h) corresponded to the scenario with the best-case CDT-containing strain ($K_{C_2} = K_{C_1}$ and $\mu_{max\text{–}C_2} = \mu_{max\text{–}C_1}$). For 75 g/L, however, the SSF process where the non-CDT containing strain was supplemented with β-glucosidase resulted in a residence time of 71 h compared to 96.75 h for the best-case CDT-containing strain. These results indicate that the introduction of a CDT transporter into SSF scenarios provides no advantage over SHF.

The residence time required for a fermentation to achieve a particular ethanol titer depends on the concentration of cells used for inoculation (0.252 g/L in this study). We studied the influence of

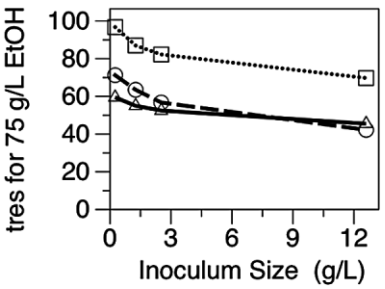

Figure 3. Sensitivity of time required to reach 75 g/L ethanol to inoculation size. The influence of inoculation size on the residence time required to produce 75 g/L ethanol was explored with scenarios where the fermentation inoculum was varied from 0.252 g/L (OD_{600} ~ 1) to 12.6 g/L (OD_{600} ~ 50). The following scenarios were investigated: SSF CDT w/$K_{C_2} = K_{C_1}$, $\mu_{max-C_2} = \mu_{max-C_1}$ C X (open squares, run 12); SSF C X BG (open circles, run 4); SHF with a 12 h hydrolysis step (open triangles, run 13).

this dependence on the relative performance of different SSF and SHF processes by plotting the residence time required to reach 75 g/L ethanol against inoculant concentration for several scenarios (Fig. 3): SSF with the non-CDT yeast supplemented with β-glucosidase (run 4), SSF with the best-case CDT yeast (run 012), and SHF with the 12 h hydrolysis step. The relative performance of the SSF runs was not affected by the inoculum size. This is consistent with the kinetics of the fermentation reaction; the rate of ethanol production is first order in yeast concentration. Thus, rate enhancements resulting from higher inoculant concentrations are identical within different SSF scenarios.

By comparison, for an SHF process with a hydrolysis step of predetermined length (e.g., 12 h), a larger inoculum size shortens only the duration of the fermentation step; the resulting reduction in overall residence time is less significant than it is within SSF. This effect is apparent in Fig. 3. As inoculum size is increased, the residence times required to reach 75 g/L ethanol decrease more rapidly in the SSF processes than in the SHF alternative. In fact, at inoculant concentrations of 12.6 g/L cells (OD_{600} ~ 50), the residence time for the SSF process conducted with a non-CDT yeast supplemented with β-glucosidase was shorter than that required by SHF with a 12 h hydrolysis step: 42.25 h compared to 45.5 h. At this high inoculum size, however, shorter residence times can likely be achieved within SHF if the hydrolysis step is shortened; the duration of this step was not optimized in the present work. Thus, while the relative performance of particular SHF and SSF scenarios is sensitive to the inoculum size, the general result remains: cellobiose-consuming yeast are unlikely to make SSF more efficient than SHF.

3.3 The influence of the cellodextrin transporter on xylose uptake rates

The CDT's role in enhancing xylose uptake by preventing glucose inhibition of xylose transport was investigated through a comparison of the times required for yeast to fully consume xylose in three scenarios: SSF with the best-case CDT-containing strain, SSF with the non-CDT-containing strain supplemented with β-glucosidase, and SHF with a 12 h hydrolysis step (Table 2). For the SHF process, the xylose consumption time was calculated by adding the time required for complete xylose consumption in the fermentation step to the 12 h required for hydrolysis. In SSF with the best CDT-containing strain, xylose was completely consumed in 27.25 h; this was significantly shorter than the 38 h required for SSF with the non-CDT-containing strain supplemented with β-glucosidase and the 37.5 h required for SHF with a 12 h hydrolysis step. As discussed above, however, the production of 75 g/L ethanol titers required residence times longer than 50 h, and all processes allowed for complete xylose utilization within this time. Moreover, we found no correlation between rapid xylose up-

Table 2. Time taken to consume xylose

Run	Conditions	B_{i-G-Xy}	$t_{cons.}$ for xylose	τ_{res} (h) 75 g/L ethanol
13	SHF with 12 h hydrolysis step; xylose added in fermentation	9 mM	37.5	59.5
4	SSF with non-CDT-containing yeast supplemented with β-glucosidase; cellulose and xylose present	9 mM	38	71
12	SSF CDT-containing yeast where $K_{C_1} = K_{C_2}$ and $\mu_{max-C_2} = \mu_{max-C_1}$; cellulose and xylose present	9 mM	27.25	96.75
13	SHF with 12 h hydrolysis step; xylose added in fermentation	90 mM	93.5	94.5
4	SSF with non-CDT-containing yeast supplemented with β-glucosidase; cellulose and xylose present	90 mM	98.75	122
12	SSF CDT-containing yeast where $K_{C_1} = K_{C_2}$ and $\mu_{max-C_2} = \mu_{max-C_1}$; cellulose and xylose present	90 mM	50	119

take and shortest residence time. Thus, the enhanced xylose consumption rates of the best-case CDT-containing strain are not beneficial when high concentrations of ethanol are desired.

Parameters describing glucose inhibition of xylose uptake by the DA24-16 strain have yet to be measured experimentally. The present work employs experimental parameters describing glucose inhibition of xylose transport in the yeast *Candida lusitaniae*, which exhibits glucose growth kinetics similar to those of *S. cerevisiae* [39]. These parameters may be incorrect for the DA24-16 strain. Thus, the cellodextrin transporter's ability to increase xylose uptake rates was further investigated with simulations where the glucose inhibition parameter ($B_{C_1\text{–Xy}}$) was increased 10-fold. In such a scenario, glucose inhibition of xylose uptake is stronger than reported in most yeast strains capable of xylose assimilation [39, 47, 48]. In the SSF run with this stronger inhibition, the optimized CDT-containing strain consumed all xylose within 50 h, a much shorter time than the 93.5 and 98.75 h required for the SHF and SSF alternative processes, respectively. Within SSF, strong glucose inhibition of xylose transport led to conditions where rapid xylose uptake correlated with short residence times; SSF with the best-case CDT yeast allowed for 75 g/L ethanol to be produced more quickly than with the non-CDT yeast. However, this correlative relationship did not hold when SHF and SSF were compared. The SHF scenario with the 12 h hydrolysis step still had the shortest residence time for a 75 g/L ethanol titer despite the longer time for complete xylose consumption.

The CDT facilitates rapid xylose consumption by alleviating glucose inhibition of xylose transport, but for high ethanol titers, this enhanced xylose utilization rate is only beneficial within SSF if glucose inhibition of xylose uptake is stronger in the DA24-16 strain than in other reported xylose-utilizing strains [39, 47, 49]. Additionally, when SSF and SHF are compared, the overall residence time for high ethanol titers is not sensitive to rapid xylose uptake, and the SHF scenario allows for shorter residence times despite leading to conditions in which xylose is consumed more slowly.

3.4 Sensitivity of the SSF/SHF comparison to values of K_{C_1} and K_{C_2}

In the present work, the Monod constant for growth on glucose (K_{C_1}) was assumed to be the lowest achievable value of the Monod constant for growth on cellobiose in an engineered CDT-containing yeast. However, reported values of K_{C_1} for yeast growth on glucose range from 0.1 to 3 mM [39, 48, 50, 51]. In our study, we used an intermediate value of 1.7 mM for K_{C_1}. To more completely explore the sensitivity of our results to K_{C_2} values that are even lower than 1.7 mM, we examined the residence times required to achieve 75 g/L ethanol in SSF with a CDT-containing strain where K_{C_2} was varied from 0.035 mM to 3.5 mM (Fig. 4). The lowest estimates of K_{C_1} for yeast are around 0.14 mM; the residence time for this value of K_{C_2} is illustrated in Fig. 4 (starred point). SSF with such a dramatically improved CDT yeast allowed for a shorter residence time than SSF with a non-CDT yeast supplemented with β-glucosidase (71 h; dashed gray line in Fig. 4). In all runs, however, the residence times were longer than the corresponding time for the SHF process with a 12 h hydrolysis step (59.5 h; black line in Fig. 4). Reductions in residence time from improvements to K_{C_2} beyond 1.7 mM were minimal and appeared to reach a limit near K_{C_2} = 0.035 mM (65 h). Thus, while performance of the CDT-containing yeast in SSF scenarios is highly sensitive to K_{C_2}, the result that SHF with a 12 h hydrolysis step leads to shorter residence times at high ethanol titers is not.

The possible influence of a lower K_{C_1} on our results was also explored (Table 1). When this K_{C_1} was lowered to 0.14 mM in runs 2, 4, and 13, the relative ordering of residence times was unchanged (2′, 4′, and 13′ in Table 1). When K_{C_2} was subsequently lowered (as above), the same result was observed. The SHF process with a 12 h hydrolysis step still allowed 75 g/L ethanol to be produced more quickly than all other processes.

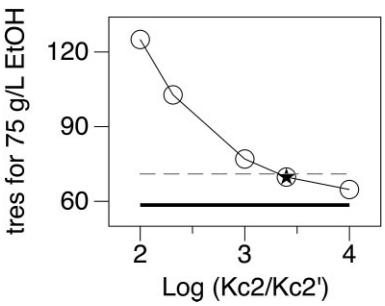

Figure 4. Sensitivity of time required to reach 75 g/L ethanol in SSF to K_{C_2}. The influence of K_{C_2} values on the residence time required to produce 75 g/L ethanol in SSF with a CDT yeast were explored. Points represent residence times for various reductions in the Monod constant associated with growth on cellobiose, which are plotted along the *x*-axis as $\log(K_{C_2}/K'_{C_2})$ where K_{C_2} = 350 mM and K'_{C_2} is an improved (lower) value of K_{C_2}. The lines correspond to the residence times required to reach 75 g/L of ethanol in SHF with a 12 h hydrolysis step (run 13; solid black line) and SSF with a non-CDT yeast supplemented with β-glucosidase (dashed gray line).

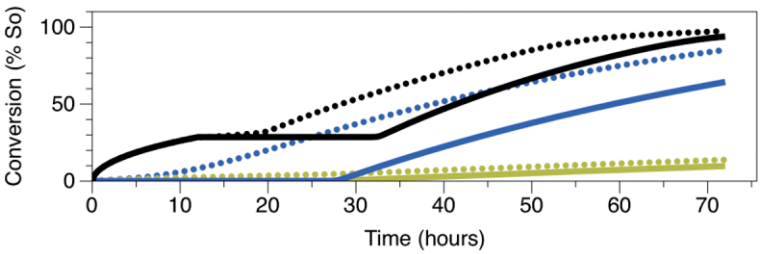

Figure 5. Sensitivity of the SSF versus SHF comparison to product inhibition. The influence of higher or lower levels of xylose inhibition was explored through a comparison of SSF with the CDT-containing yeast (run 2), SSF with the best-case CDT-containing yeast (run 12), and SHF with a 12 h hydrolysis step (run 13). Low inhibition (low Xi) corresponds to runs in which $K_{I=\text{xyl}} = K_{i-C_1} = 295$ mM. High inhibition (high Xi) corresponds to runs in which $K_{i-\text{Xy}} = K_{i-C_2}$ for each enzyme. Lines correspond to conversion profiles for the following conditions: SSF CDT C X high Xi (solid yellow line); SSF CDT w/$K_{C_2} = K_{C_1}$, $\mu_{\text{max}-C_2} = \mu_{\text{max}-C_1}$ high Xi (solid blue line); 12-H SHF C high Xi (solid black line); SSF CDT C X low Xi (dotted yellow line); SSF CDT w/$K_{C_2} = K_{C_1}$, $\mu_{\text{max}-C_2} = \mu_{\text{max}-C_1}$ low Xi (dotted blue line); 12-H SHF C low Xi (dotted black line).

3.5 Sensitivity of the SSF/SHF comparison to glucose, cellobiose, and xylose inhibition

The potential advantages of SSF and SHF may be sensitive to inhibition of cellulase enzymes by glucose, cellobiose, and xylose. Xylose inhibition in particular is not well studied; there are no directly measured inhibition parameters describing the impact of this sugar on cellulase enzymes. The influence of xylose inhibition was explored through a comparison of cellulose conversion profiles generated by three processes simulated with low and high estimates of xylose inhibition parameters: SSF with the CDT-containing yeast, SSF with the best-case CDT-containing yeast, and SHF with a 12 h hydrolysis step (runs 2, 12, and 13 in Table 1).

Parameter values describing the competitive inhibition of cellulase enzymes by xylose ($K_{i-\text{Xy}}$) were estimated from published measurements of cellulase inhibition by other sugars. In the simulations discussed in 3.1–3.5, equilibrium constants for competitive xylose inhibition were set equal to measured equilibrium constants for glucose inhibition, which ranged from 17–31 mM. Reported measurements of glucose inhibition, however, are inconsistent. A study by Phillippidis et al. reported a K_{i-C_1} value of 295 mM for a similar mixture of *Trichoderma* sp. enzymes [52]. The implications of such values on the results of this work were investigated with runs where glucose and xylose inhibition parameters were set equal to this higher value ($K_{i-\text{Xy}} = K_{i-C_1} = 295$ mM). These runs represent a low xylose inhibition scenario.

A high xylose inhibition scenario was also simulated. Xylan hydrolyzate is not necessarily composed entirely of xylose, but can be dominated by xylo-oligomers that have been shown to be as inhibitory of cellulase enzymes as cellobiose [5]. To investigate the implications of xylan hydrolyzate that is strongly inhibitory, competitive equilibrium constants for xylose inhibition were equated with the analogous constants for cellobiose inhibition ($K_{i-\text{Xy}} = K_{i-C_2}$ for each enzyme).

Cellulose conversion profiles over 72 h are reported in Fig. 5. The cellulose conversion profile for the CDT-containing yeast in the SSF scenario was not significantly affected by xylose inhibition parameters. At reduced levels of xylose and glucose inhibition, the SHF process resulted in 15% higher conversion at 72 h than the SSF process with the best CDT-containing yeast; at the higher level of xylose inhibition, the SHF process led to a 25% higher conversion. Thus, SHF outperformed SSF at low and high levels of xylose inhibition, indicating that the results of this work are insensitive to the values of the parameters used to describe xylose inhibition.

3.6 A Best-case scenario for cellobiose consumption

To assess the ability of a CDT-containing yeast to achieve high ethanol titers, we ran the model with $K_{C_2} = 0$, $B_{C_1-C_2} = 0$, and $\mu_{\text{max}-C_2} = 0.5$ h^{-1} (run 19 in Table 1). Under such circumstances, cellobiose uptake can be represented by the following equation:

$$\text{rate of cellobiose uptake} = -\left(\frac{1}{Y_{X/C_2}}\right)\left(\mu_{\text{max}-C_2}\right)\left(1-\frac{[\text{Ethanol}]}{K_{i-\text{Eth}-X}}\right)X \quad (12)$$

Here, uptake of cellobiose (and growth on cellobiose) is governed only by the maximum specific growth rate of *S. cerevisiae* and inhibition by ethanol, and is zeroth order in cellobiose. For such a strain, the residence time required to achieve 75 g/L of ethanol was 62.25 h, which is still 4.6% higher than the residence time for SHF with a 12 h hydrolysis step. The same result was obtained in the set of runs where $K_{C_1} = 0.14$ mM (run 19′ in Table 1). Accordingly, improvements to the cel-

lobiose assimilation pathway are not likely to lead to a strain of yeast that allows high ethanol titers to be reached more quickly in SSF than in SHF.

3.7 Collection of parameter values

Some of the parameter values for the microbial growth model employed in the present analysis were not available in the literature and had to be estimated from limited datasets and non-*Saccharomyces* yeast strains. As discussed above, the conclusions of the present work are not sensitive to these parameters, but the model-predicted performance of any particular strain is. Future work to engineer yeast strains capable of xylose and cellobiose assimilation should involve attempts to accurately measure kinetic parameters for growth on these substrates ($K_{\text{substrate}}$, $\mu_{\text{max-substrate}}$, $B_{C_1\text{-substrate}}$).

4 Concluding remarks

We combined a detailed mechanistic kinetic model of cellulase-catalyzed hydrolysis with a multi-substrate model of microbial growth to investigate the ability of cellobiose utilizing *S. cerevisiae* to facilitate cellulase hydrolysis and improve ethanol titers using SSF. The model showed that an existing strain with this capability (DA24-16) is not as effective at enhancing rates of cellulose hydrolysis or ethanol production as a non-cellobiose-utilizing alternative supplemented with β-glucosidase. However, lowering the Monod constant for growth on cellobiose would enable DA24-16 to produce ethanol from cellulose and xylose nearly as rapidly as the non-cellobiose-utilizing alternative. Strategies to lower the Monod constant include increasing transporter expression and/or increasing the rate of intracellular cellobiose hydrolysis. Such a best-case CDT strain would likely reduce, but not eliminate, the β-glucosidase requirement.

By relieving glucose inhibition of xylose uptake, the CDT allowed xylose to be consumed more quickly in CDT yeast than in non-CDT yeast with the same xylose assimilation pathway machinery. Rapid xylose uptake, however, did not result in short residence times for producing 75 g/L ethanol unless glucose inhibition of xylose uptake was assumed to be higher in the DA24-16 strain than for most other xylose-consuming yeast strains; and, under such circumstances, this correlation existed only in SSF scenarios. The SHF scenario with the 12 h hydrolysis step required more time for complete xylose utilization but allowed high ethanol titers to be reached more quickly than in SSF processes, regardless of the level of glucose inhibition of xylose uptake.

Improvements to the cellobiose utilization system of the DA24-16 strain are unlikely to result in SSF residence times that are shorter than those of SHF processes. Our simulations showed that SHF with a 12 h hydrolysis step allowed 75 g/L ethanol titers to be reached more quickly than all SSF processes addressed in this work. A technoeconomic analysis is necessary to determine whether or not the longer residence times required in SSF with optimized CDT-containing strains of *S. cerevisiae* could allow for a net cost savings resulting from the elimination or reduction in β-glucosidase requirements.

In an SHF process, improved cellobiose-utilizing strains could still be useful. If cellulases that are insensitive to cellobiose are developed, there would be no need for β-glucosidase in the hydrolysis step; and enzyme cost would be reduced. In this scenario, any organism capable of rapid cellobiose consumption would be advantageous in the fermentation step, which would contain a high concentration of cellobiose.

We thank Professor Yong-Su Jin and Jonathan M. Galazka for helpful discussion. J. M. F., S. E. L., H. W. B, and D. S. C designed research. J. M. F. and S. E. L. wrote Fortran code. J. M. F. carried out modeling runs and analyzed data. J. M. F., S. E. L., H. W. B., and D. S. C. wrote paper. J. M. F. is a recipient of a National Science Foundation predoctoral fellowship. This work was funded by award 50000029463 from the Energy Biosciences Institute to D. S. C. and H. W. B.

The authors declare no conflict of interest.

5 References

[1] Lynd, L. R., Cushman, J. H., Nichols, R. J., Wyman, C. E., Fuel ethanol from cellulosic biomass. *Science* 1991, *251*, 1318–1323.

[2] Lynd, L. R., van Zyl, W. H., McBride, J. E., Laser, M., Consolidated bioprocessing of cellulosic biomass: An update. *Curr. Opin. Biotechnol.* 2005, *16*, 577–583.

[3] Wyman, C. E., Hinman, N. D., Ethanol – fundamentals of production from renewable feedstocks and use as a transportation fuel. *Appl. Biochem. Biotechnol.* 1990, *24–25*, 735–753.

[4] Carroll, A., Somerville, C., Cellulosic biofuels. *Annu. Rev. Plant Biol.* 2009, *60*, 165–182.

[5] Qing, Q., Yang, B., Wyman, C. E., Xylooligomers are strong inhibitors of cellulose hydrolysis by enzymes. *Bioresource Technol.* 2010, *101*, 9624–9630.

[6] Roberto, I. C., Mussatto, S. I., Rodrigues, R. C. L. B., Dilute-acid hydrolysis for optimization of xylose recovery from rice straw in a semi-pilot reactor. *Ind. Crop. Prod.* 2003, *17*, 171–176.

[7] Holtzapple, M., Cognata, M., Shu, Y., Hendrickson, C., Inhibition of Trichoderma-Reesei cellulase by sugars and solvents. *Biotechnol. Bioeng.* 1990, *36*, 275–287.

[8] Ha, S. J., Galazka, J. M., Kim, S. R., Choi, J. H. et al., Engineered *Saccharomyces cerevisiae* capable of simultaneous cellobiose and xylose fermentation. *Proc. Natl. Acad. Sci. USA* 2011, *108*, 504–509.

[9] Wahlbom, C. F., Otero, R. R. C., van Zyl, W. H., Hahn-Hagerdal, B., Jonsson, L. J., Molecular analysis of a Saccharomyces cerevisiae mutant with improved ability to utilize xylose shows enhanced expression of proteins involved in transport, initial xylose metabolism, and the pentose phosphate pathway. *Appl. Environ. Microb.* 2003, *69*, 740–746.

[10] Grootjen, D. R. J., Vanderlans, R. G. J. M., Luyben, K. C. A. M., Conversion of glucose xylose mixtures by Pichia-stipitis under oxygen-limited conditions. *Enzyme Microb. Technol.* 1991, *13*, 648–654.

[11] Gardonyi, M., Jeppsson, M., Liden, G., Gorwa-Grausland, M. F., Hahn-Hagerdal, B., Control of xylose consumption by xylose transport in recombinant Saccharomyces cerevisiae. *Biotechnol. Bioeng.* 2003, *82*, 818–824.

[12] Saitoh, S., Tanaka, T., Kondo, A., Breeding of industrial diploid yeast strain with chromosomal integration of multiple beta-glucosidase genes. *J. Biosci. Bioeng.* 2008, *106*, 594–597.

[13] Shen, Y., Zhang, Y., Ma, T., Bao, X. M. et al., Simultaneous saccharification and fermentation of acid-pretreated corncobs with a recombinant Saccharomyces cerevisiae expressing beta-glucosidase. *Bioresource Technol.* 2008, *99*, 5099–5103.

[14] Rajoka, M. I., Bashir, A., Hussain, S. R. A., Ghauri, M. T. et al., Cloning and expression of beta-glucosidase genes in *Escherichia coli* and *Saccharomyces cerevisiae* using shuttle vector pYES 2.0. *Folia Microbiol.* 1998, *43*, 129–135.

[15] Galazka, J. M., Tian, C. G., Beeson, W. T., Martinez, B. et al., Cellodextrin transport in yeast for improved biofuel production. *Science* 2010, *330*, 84–86.

[16] Humbird, D., Mohagheghi, A., Dowe, N., Schell, D. J., Economic impact of total solids loading on enzymatic hydrolysis of dilute acid pretreated corn stover. *Biotechnol. Prog.* 2010, *26*, 1245–1251.

[17] Levine, S. E., Fox, J. M., Blanch, H. W., Clark, D. S., A mechanistic model of the enzymatic hydrolysis of cellulose. *Biotechnol. Bioeng.* 2010, *107*, 37–51.

[18] Hamelinck, C. N., van Hooijdonk, B., Faaij, A. P., Ethanol from lignocellulosic biomass: Techno-economic performance in short-, middle-, and long-term. *Biomass Bioenergy* 2005, *28*, 384–410.

[19] Lan, W., Liu, C. F., Sun, R. C., Fractionation of bagasse into cellulose, hemicelluloses, and lignin with ionic liquid treatment followed by alkaline extraction. *J. Agric. Food Chem.* 2011, *59*, 8691–8701.

[20] Morinelly, J. E., Jensen, J. R., Browne, M., Co, T. B., Shonnard, D. R., Kinetic characterization of xylose monomer and oligomer concentrations during dilute acid pretreatment of lignocellulosic biomass from forests and switchgrass. *Ind. Eng. Chem. Res.* 2009, *48*, 9877–9884.

[21] Banerjee, G., Car, S., Scott-Craig, J. S., Borrusch, M. S. et al., Synthetic enzyme mixtures for biomass deconstruction: Production and optimization of a core set. *Biotechnol. Bioeng.* 2010, *106*, 707–720.

[22] Akpinar, O., Levent, O., Bostanci, S., Bakir, U., Yilmaz, L., The optimization of dilute acid hydrolysis of cotton stalk in xylose production. *Appl. Biochem. Biotechnol.* 2011, *163*, 313–325.

[23] Kadam, K. L., Rydholm, E. C., McMillan, J. D., Development and validation of a kinetic model for enzymatic saccharification of lignocellulosic biomass. *Biotechnol. Prog.* 2004, *20*, 698–705.

[24] Chen, Y., Dong, B., Qin, W., Xiao, D., Xylose and cellulose fractionation from corncob with three different strategies and separate fermentation of them to bioethanol. *Bioresour Technol.* 2010, *101*, 7005–7010.

[25] Podkaminer, K. K., Shao, X. J., Hogsett, D. A., Lynd, L. R., Enzyme inactivation by ethanol and development of a kinetic model for thermophilic simultaneous saccharification and fermentation at 50 degrees C with thermoanaerobacterium saccharolyticum ALK2. *Biotechnol. Bioeng.* 2011, *108*, 1268–1278.

[26] van Zyl, J. M., van Rensburg, E., van Zyl, W. H., Harms, T. M., Lynd, L. R., A Kinetic model for simultaneous saccharification and fermentation of avicel with *Saccharomyces cerevisiae*. *Biotechnol. Bioeng.* 2011, *108*, 924–933.

[27] Sun, Y., Cheng, J. Y., Hydrolysis of lignocellulosic materials for ethanol production: A review. *Bioresource Technol.* 2002, *83*, 1–11.

[28] Houghton, J., Weatherwax, S., Ferrel, J., Breaking the biological barriers to cellulosic ethanol: A joint research agenda, *US Dep. Energy* 2006, DOE/SC-0095.

[29] Baker, J. O., Ehrman, C. I., Adney, W. S., Thomas, S. R., Himmel, M. E., Hydrolysis of cellulose using ternary mixtures of purified celluloses. *Appl. Biochem. Biotechnol.* 1998, *70–72*, 395–403.

[30] Accellerase Duet Product Information Sheet. Genencor, A Danisco Division. 2010, 01-2010.indd.

[31] Chauve, M., Mathis, H., Huc, D., Casanave, D. et al., Comparative kinetic analysis of two fungal beta-glucosidases. *Biotechnol. Biofuels* 2010, *3*, 3.

[32] Levine, S. E., Fox, J. M., Blanch, H. W., Clark, D. S., A mechanistic model for rational design of optimal cellulase mixtures. *Biotechnol. Bioeng.* 2011, *108*, 2561–2570.

[33] Holtzapple, M. T., Caram, H. S., Humphrey, A. E., The Hch-1 model of enzymatic cellulose hydrolysis. *Biotechnol. Bioeng.* 1984, *26*, 775–780.

[34] Okazaki, M., Mooyoung, M., Kinetics of enzymatic-hydrolysis of cellulose – analytical description of a mechanistic model. *Biotechnol. Bioeng.* 1978, *20*, 637–663.

[35] Peri, S., Karra, S., Lee, Y. Y., Karim, M. N., Modeling intrinsic kinetics of enzymatic cellulose hydrolysis. *Biotechnol. Prog.* 2007, *23*, 626–637.

[36] Wald, S., Wilke, C. R., Blanch, H. W., Kinetics of the enzymatic-hydrolysis of cellulose. *Biotechnol. Bioeng.* 1984, *26*, 221–230.

[37] Ghose, T. K., Tyagi, R. D., Rapid ethanol fermentation of cellulose hydrolysate .1. Batch versus continuous systems. *Biotechnol. Bioeng.* 1979, *21*, 1387–1400.

[38] Stephanopoulos, G., Challenges in engineering microbes for biofuels production. *Science* 2007, *315*, 801–804.

[39] Kwon, Y. J., Engler, C. R., Kinetic models for growth and product formation on multiple substrates. *Biotechnol. Bioprocess Eng.* 2005, *10*, 587–592.

[40] Galazka, J. M., Cate, J. H., A new diet for yeast to improve biofuel production. *Bioeng. Bugs.* 2011, *2*, 199–202.

[41] Warner, J. R., The economics of ribosome biosynthesis in yeast. *Trends Biochem. Sci.* 1999, *24*, 437–440.

[42] French, S. L., Osheim, Y. N., Cioci, F., Nomura, M., Beyer, A. L., In exponentially growing *Saccharomyces cerevisiae* cells, rRNA synthesis is determined by the summed RNA polymerase I loading rate rather than by the number of active genes. *Mol. Cell. Biol.* 2003, *23*, 1558–1568.

[43] Kief, D. R., Warner, J. R., Coordinate control of syntheses of ribosomal ribonucleic-acid and ribosomal-proteins during nutritional shift-up in *Saccharomyces cerevisiae*. *Mol. Cell. Biol.* 1981, *1*, 1007–1015.

[44] Elbing, K., Larsson, C., Bill, R. M., Albers, E. et al., Role of hexose transport in control of glycolytic flux in Saccharomyces cerevisiae. *Appl. Environ. Microbiol.* 2004, *70*, 5323–5330.

[45] Button, D. K., Robertson, B., Gustafson, E., Zhao, X., Experimental and theoretical bases of specific affinity, a cytoarchitecture-based formulation of nutrient collection proposed to supercede the Michaelis–Menten paradigm of microbial kinetics. *Appl. Environ. Microbiol.* 2004, *70*, 5511–5521.

[46] Button, D. K., Kinetics of nutrient-limited transport and microbial growth. *Microbiol. Rev.* 1985, *49*, 270–297.

[47] Hahn-Hagerdal, B., Wahlbom, C. F., Gardonyi, M., van Zyl, W. H. et al., Metabolic engineering of *Saccharomyces cerevisiae* for xylose utilization. *Adv. Biochem. Eng. Biotechnol.* 2001, *73*, 53–84.

[48] Morales-Rodriguez, R., Gernaey, K. V., Meyer, A. S., Sin, G., A mathematical model for simultaneous saccharification and co-ferentation (SSCF) of C6 and C5 sugars. *Chin. J. Chem. Eng.* 2010, *19*, 185–191.

[49] Saloheimo, A., Rauta, J., Stasyk, O. V., Sibirny, A. A. et al., Xylose transport studies with xylose-utilizing *Saccharomyces cerevisiae* strains expressing heterologous and homologous permeases. *Appl. Microbiol. Biotechnol.* 2007, *74*, 1041–1052.

[50] Blanch, H. W., Clark, D. S., *Biochemical Engineering*, M. Dekker, New York 1997.

[51] Postma, E., Scheffers, W. A., van Dijken, J. P., Kinetics of growth and glucose transport in glucose-limited chemostat cultures of *Saccharomyces cerevisiae* CBS 8066. *Yeast* 1989, *5*, 159–165.

[52] Philippidis, G. P., Smith, T. K., Wyman, C. E., Study of the enzymatic-hydrolysis of cellulose for production of fuel ethanol by the simultaneous saccharification and fermentation process. *Biotechnol. Bioeng.* 1993, *41*, 846–853.

